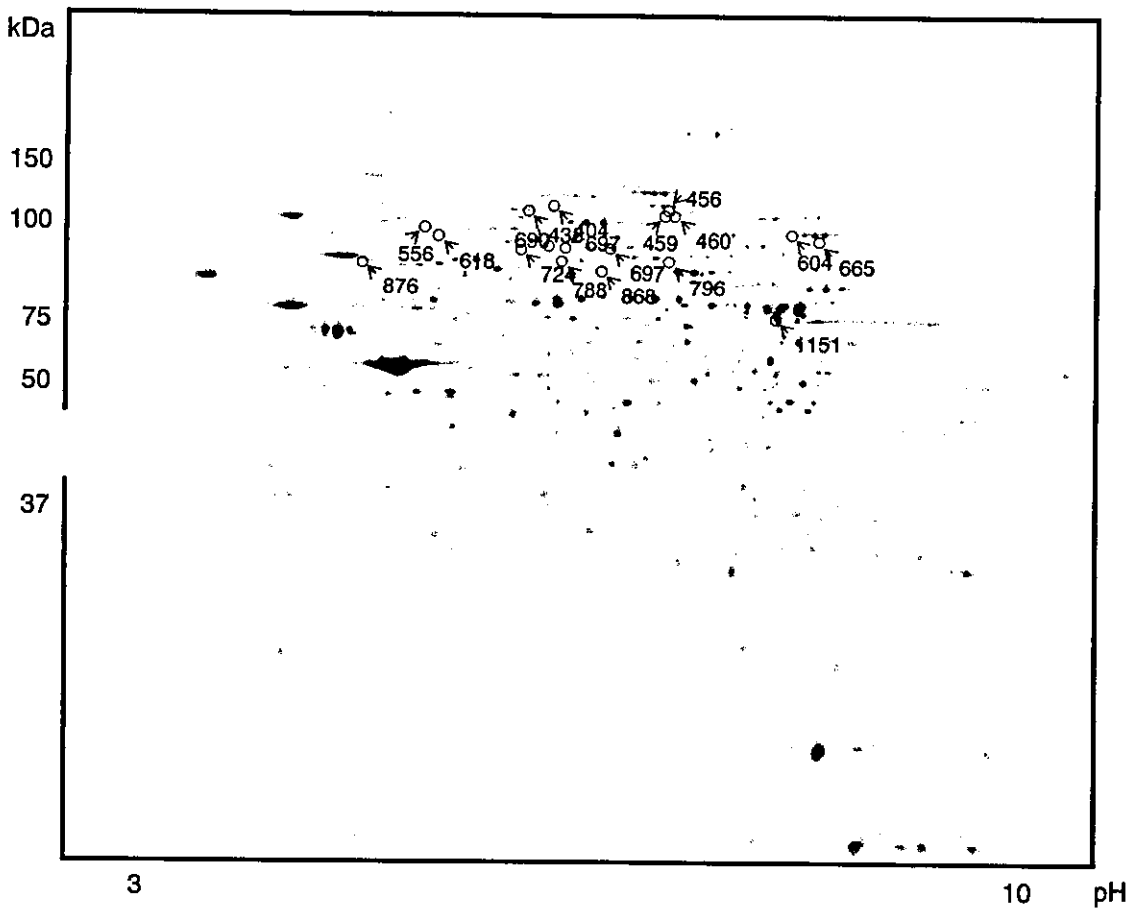

図 8. 2D image of protein expression differences between soluble fractions from lupus model mice (MRL-lpr/lpr) and control mouse (MRL-+/+) kidneys. Black highlights indicate protein spots, which were up- or down-regulated in MRL-lpr/lpr mice compared to MRL-+/+ control mice.

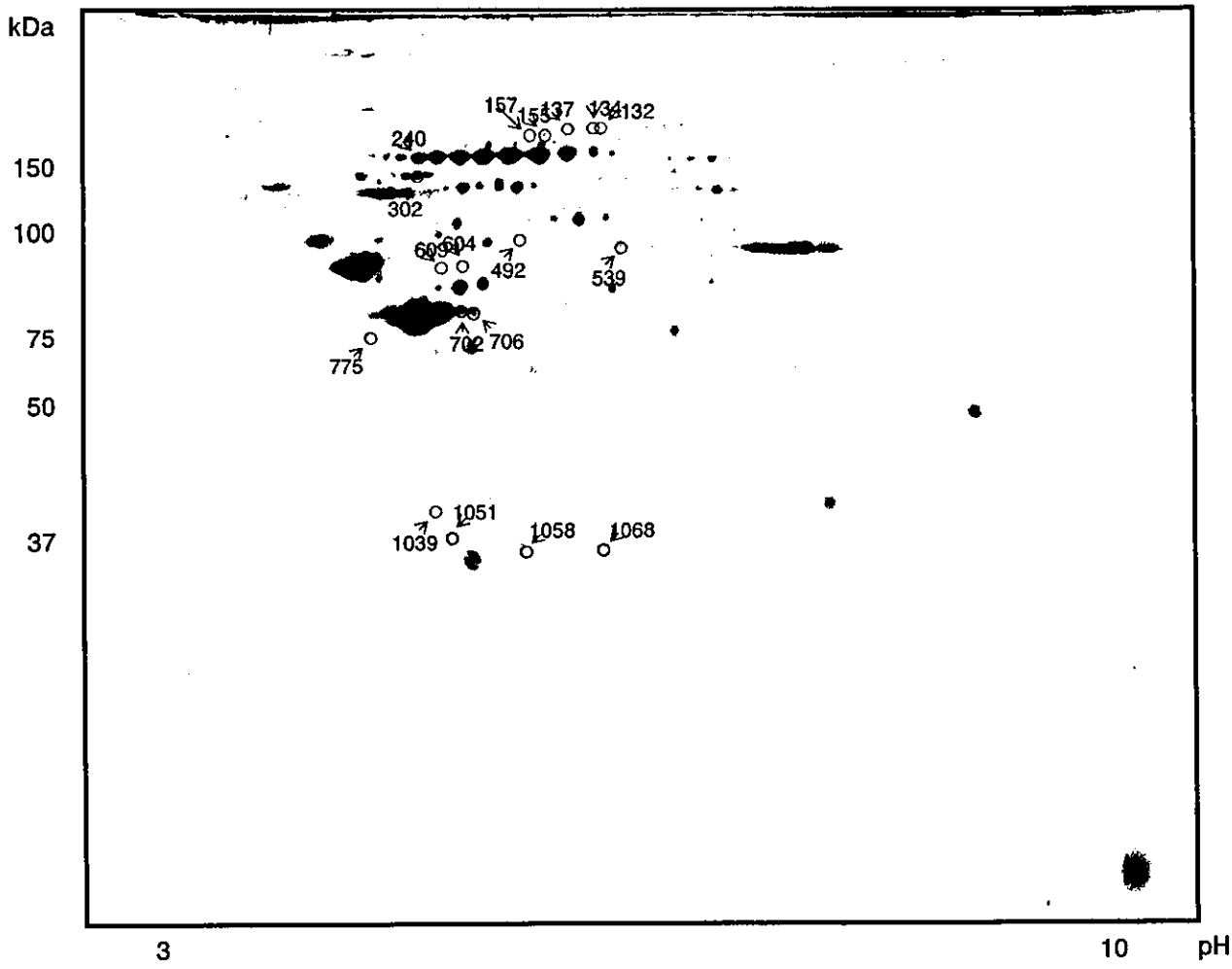

図9. 2D image of protein expression differences between insoluble fractions from lupus model mice (MRL-lpr/lpr) and control mouse (MRL-+/+) kidneys. Black highlights indicate protein spots, which were up- or down-regulated in MRL-lpr/lpr mice compared to MRL-+/+ control mice.

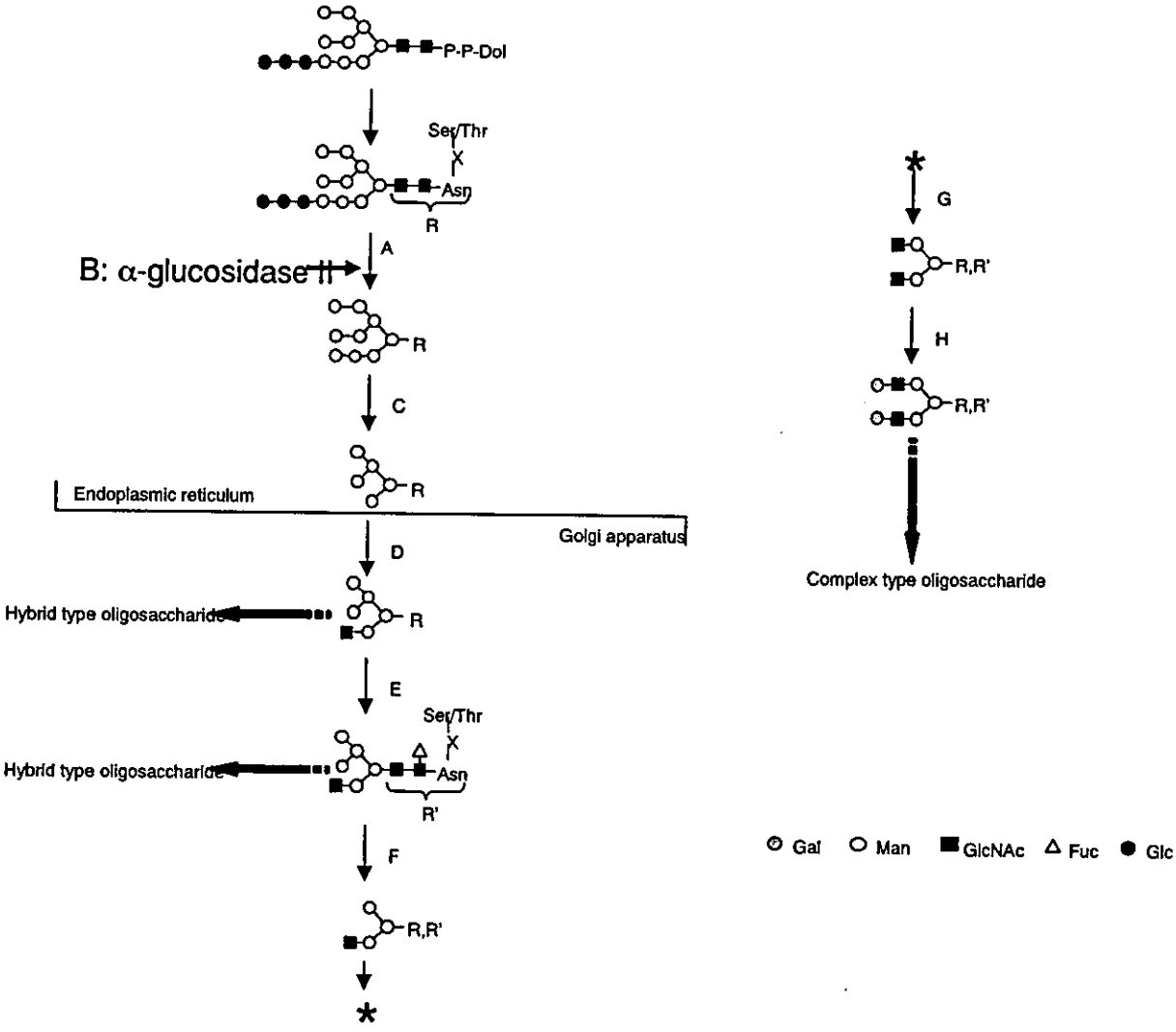

図 10 Biosynthetic pathway of *N*-linked oligosaccharide. P; phosphate, Dol; dolichol, A; α-glucosidase I, B; α-glucosidase II, C; α-mannosidase, D; *N*-acetylglucosaminyltransferase I, E; α-1,6-fucosyltransferase, F; α-mannosidase II, G; *N*-acetylglucosaminyltransferase II, H; β-1,4-galactosyltransferase

表 6 Differentially expressed protin spots in lpr/lpr mouse soluble fraction compared to +/+ mouse

Spot No.	Protein Name	NCBI accession No.	*t*-test ($p<0.05$)	Average Ratio
404	α-glucosidase II α-subunit	6679891	0.0230	-1.30
438	α-glucosidase II α-subunit	6679891	0.0470	-1.20
459	oxoglutarate dehydrogenase	15489120	0.0080	1.35
460	oxoglutarate dehydrogenase	15489120	0.0045	1.26
556	interfelon-inducible protein 10 receptor	20984919	0.0240	1.21
604	aconitase II	18079339	0.0450	1.41
665	metastasis-associated protein MTA1	28411669	0.0180	-1.24
690	thimet oligopeptidase I	31981237	0.0019	1.15
693	ezrin	6678571	0.0230	1.15
697	ezrin	6678571	0.0010	1.10
788	transglutaminase type 1	7081495	0.0053	1.39
796	β-glucuronidase precursor	114964	0.0049	-1.09
868	unamed protein product	26336937	0.0220	-1.27
876	PDZ domain containing I	10946938	0.0460	1.19

表 7 Differentially expressed protin spots in lpr/lpr mouse insoluble fraction compared to +/+ mouse

Spot No.	Protein Name	NCBI accession No.	*t*-test ($p<0.05$)	Average Ratio
132	nidogen1	6754854	0.016	1.28
134	nidogen1	6754854	0.006	1.40
137	nidogen1	6754854	0.045	1.48
155	α-glucosidase II α-subunit	6754854	0.033	-1.19
162	α-glucosidase II α-subunit	6679891	0.019	-1.31
240	meprin	6679891	0.042	-1.53
302	NADH dehydrogenase Fe-S protein 1	31982199	0.048	1.25
492	vacuolar H+-ATPase	21704020	0.022	1.23
539	D-lactate dehydorogenase	162723	0.017	1.24
604	ATPS	23506790	0.011	-1.29
609	ATPS	2623222	0.034	-1.13
702	laminC	2623222	0.015	1.20
775	tropomoduline3	1794159	0.041	1.31
1039	metaxin2	8394460	0.001	1.36
1051	NADPH dehydrogenase	13124347	0.022	1.39
1058	glutation peroxydase 3 (GPx3)	20900762	0.018	2.30
1068	glutation peroxydase 3 (GPx3)	25011841	0.012	2.34

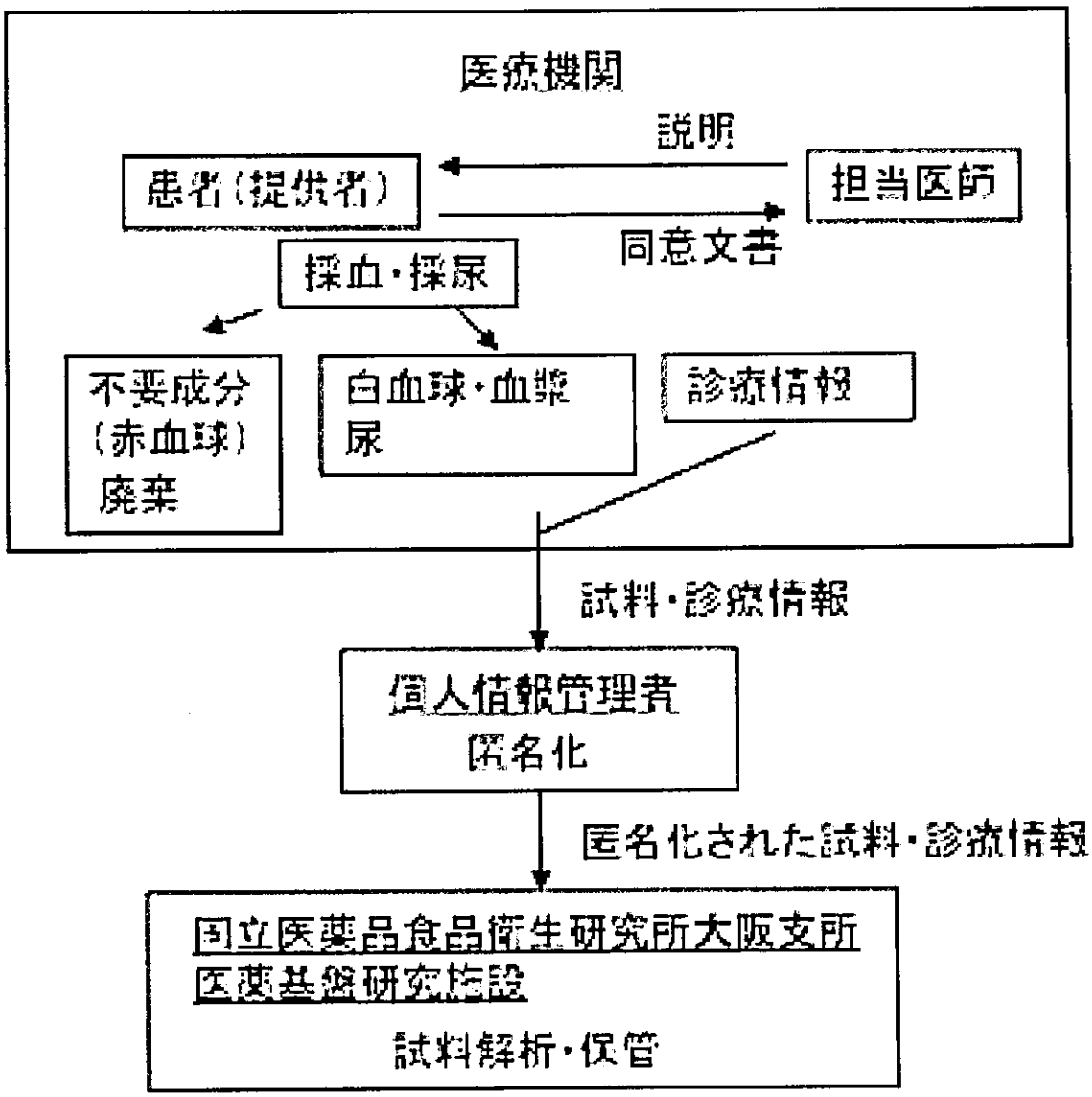

図11　臨床検体の受入体制

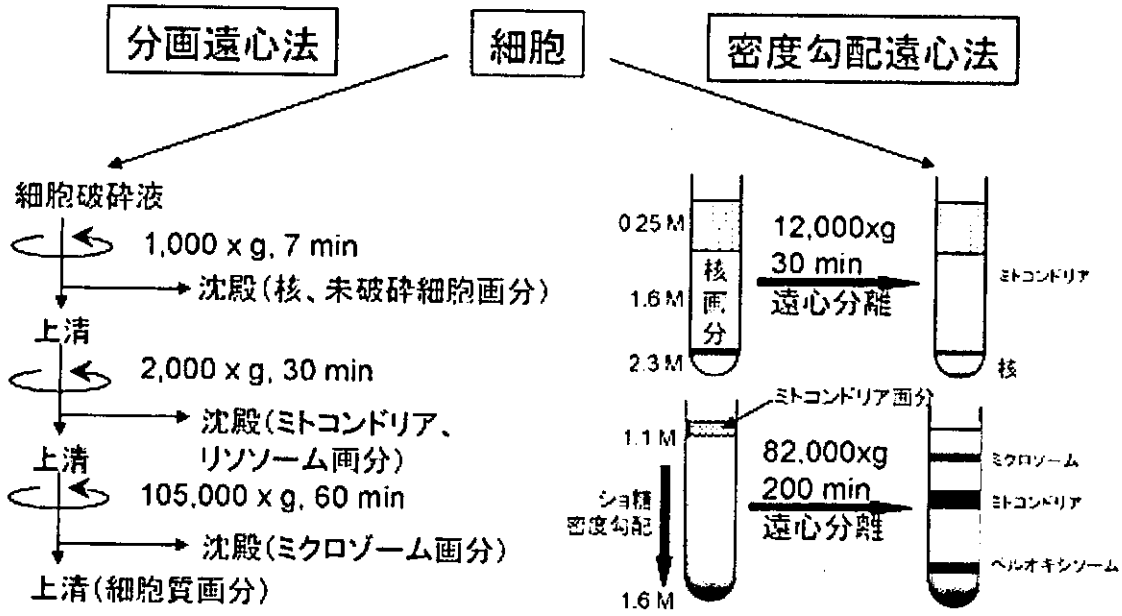

図12 組織・細胞からのたんぱく質の分離・抽出条件検討

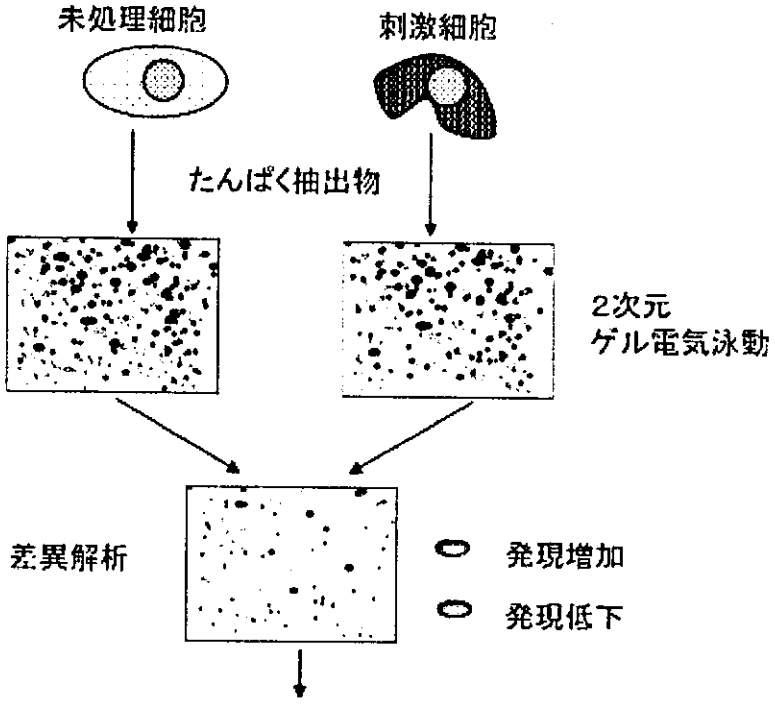

図13 2次元ゲル電気泳動(2DGE)によるたんぱく質の分離・精製 と比較評価

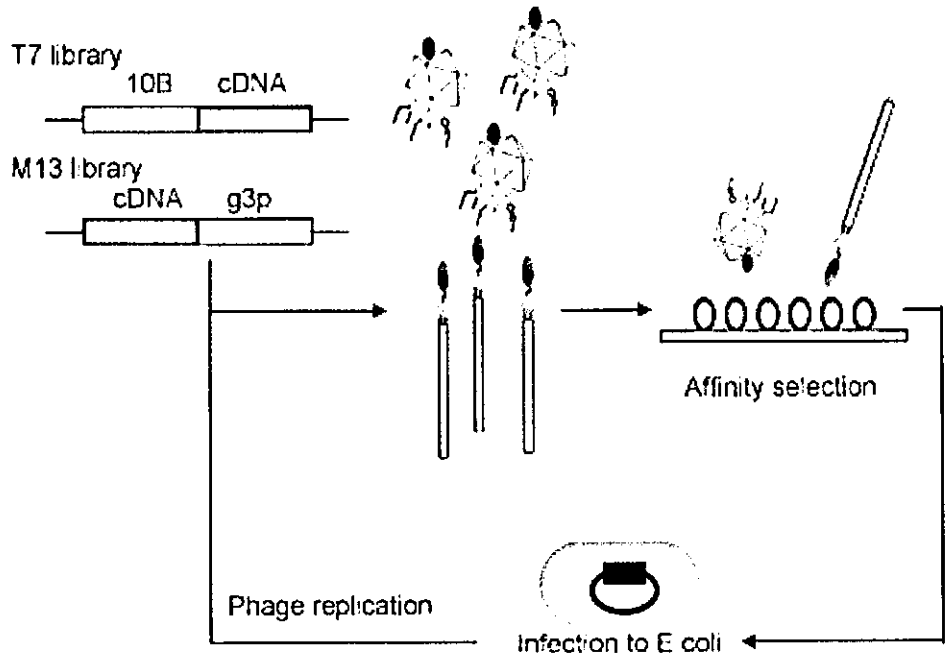

図14　疾患関連細胞cDNAファージディスプレイライブラリによる相互作用分子の探索

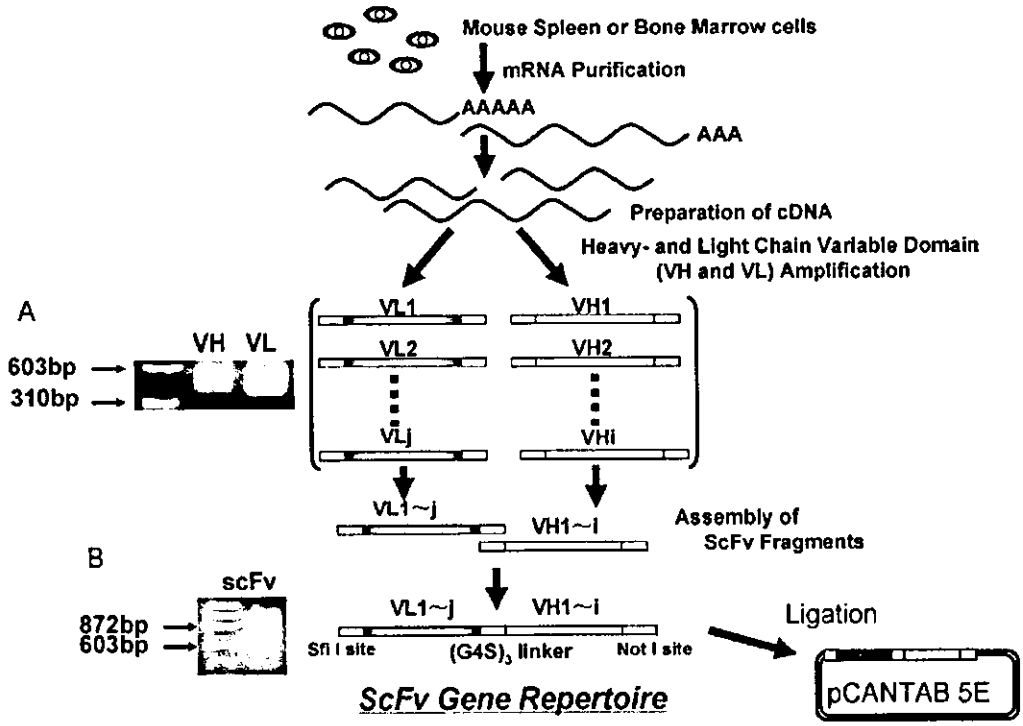

図15　マウスcDNAからのVL遺伝子とVH遺伝子の増幅

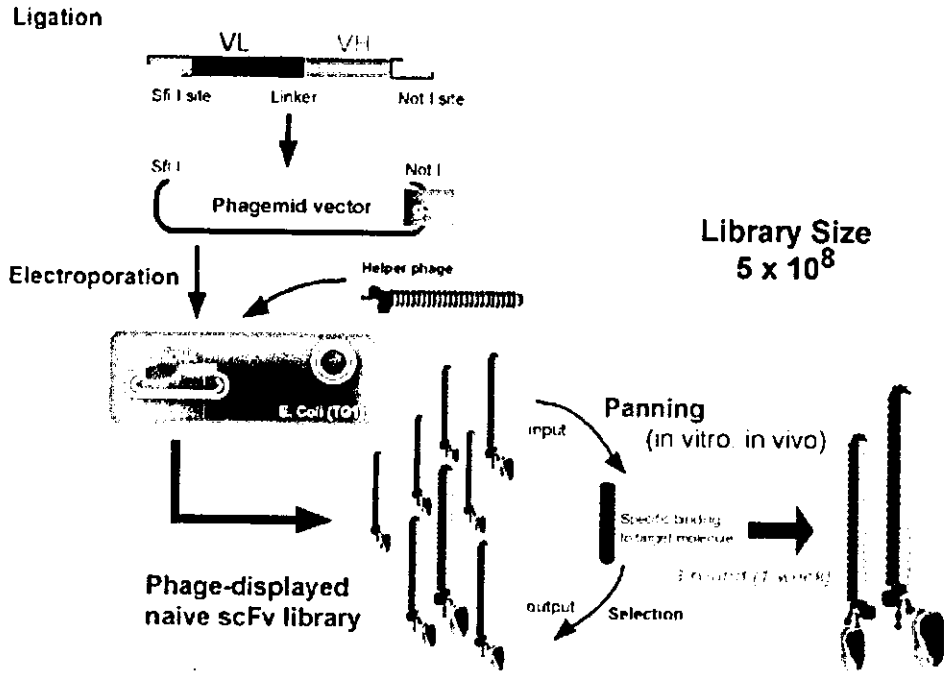

図16 ナイーブscFvを表面提示したファージライブラリの作製

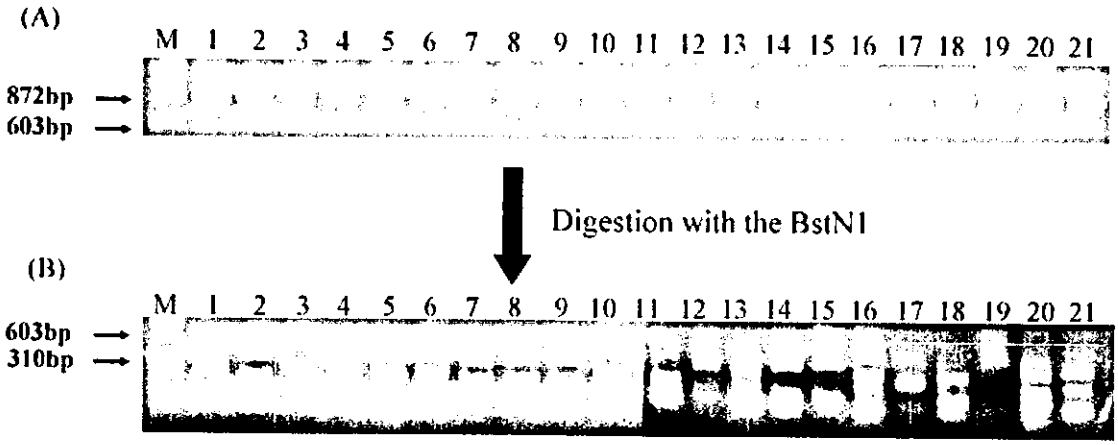

図17 BstN IによるscFv遺伝子のフィンガープリント解析

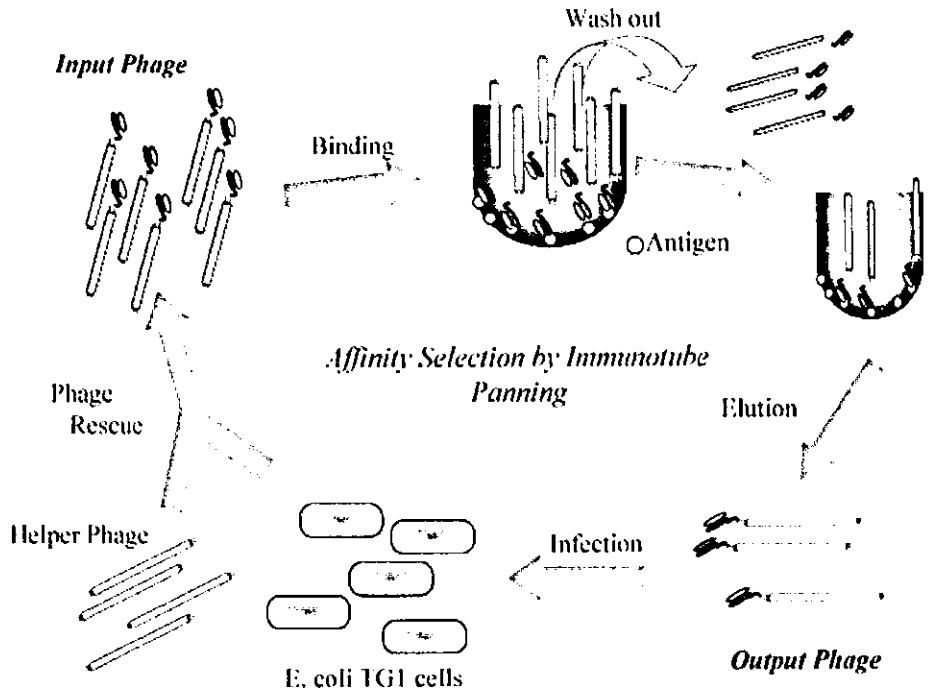

図18 種々抗原に対するパンニング

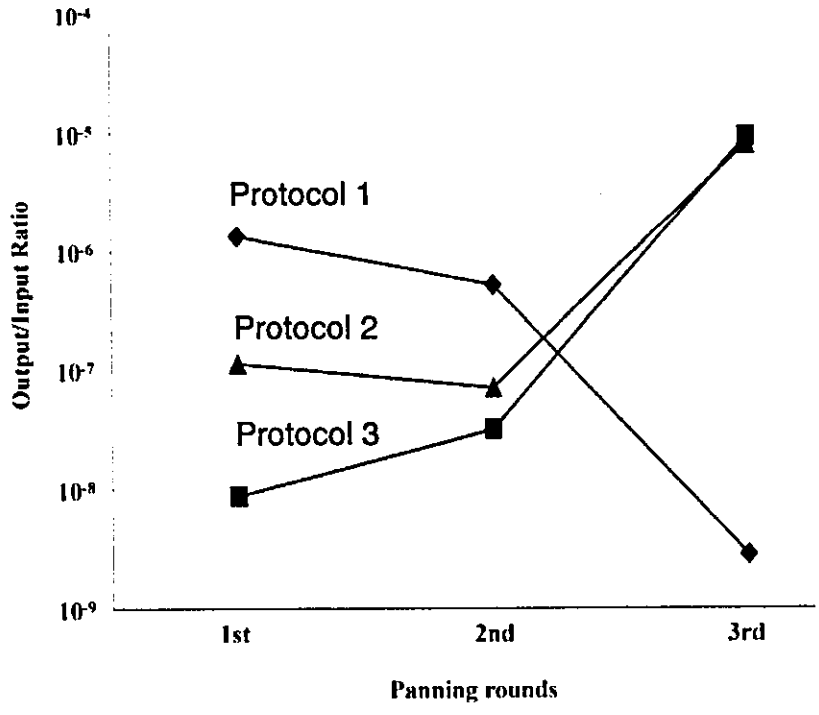

図19 パンニングによるルシフェラーゼに結合するscFv提示ファージの濃縮（パンニング条件の設定）

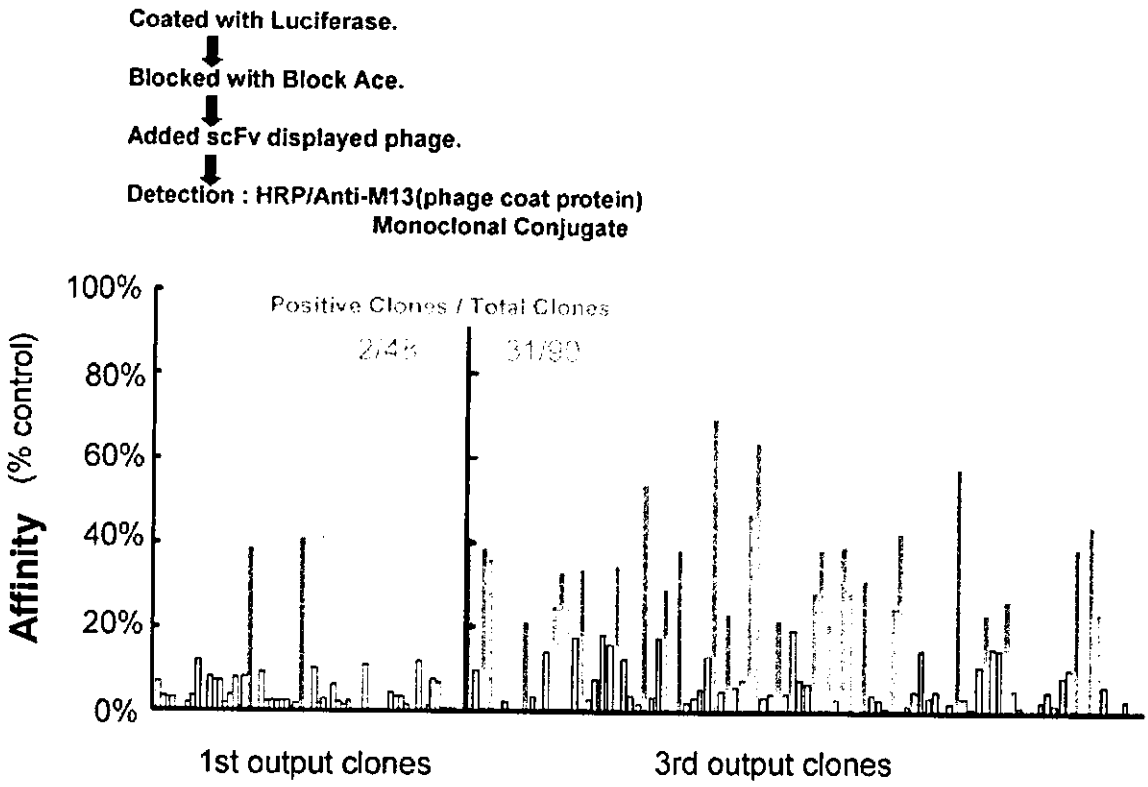

図20　ルシフェラーゼに対するファージELISA

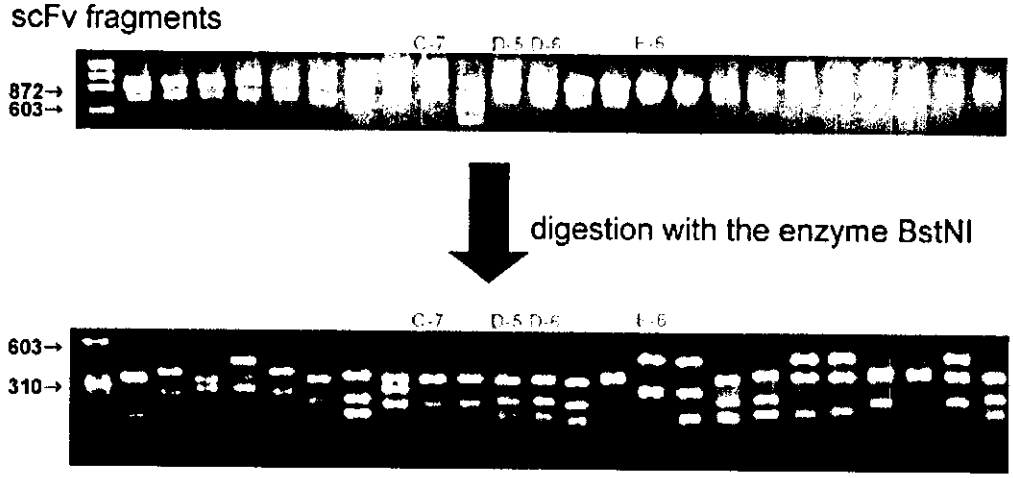

図21　BstN Iを用いたフィンガープリント解析

表8 ルシフェラーゼに対する種々モノクローナルscFv のアミノ酸シーケンス

	VL							Linker
	FR1	CDR1	FR2	CDR2	FR3	CDR3	FR4	(G4S)3
C-7	DIQMMQSTSSLSASL GDRVTISC	RTSQDI NTYLN	WYQQKPDG TVKLLIY	YTSRL HS	GVPSRFSGSGSGTDYSLTISN LEQEDIATYFC	QQGNTL PLT	FGAGTK LELKR	GGGGSGGGG SGGGGS
D-5	DIVITQSPAILSVSPGE RVSFSC	RASQSI GTSIH	WYQQRTNG SPRLLIE	YASE SIS	GIPSRFSGSGSGTDFTLSINSV ESEDIADYYC	QQSNS WPTT	FGAGTK LTVL	GGGGSGGGG SGGGGS
D-6	DIQMTQSPVILSVSPE GERVSFSC	RASQSI GTSIH	WYQQRING PPRPLIK	YASE SIS	RIPSRFSGSGSGTDFTLSINSV ESEDIADYYC	QQSNS WPALT	FGAGTK LEIKR	GGGGSGGGG SGGGGS
E-6	DILLTQSPVILSVSPG ERVSFSC	RASQNI GTSIH	WYQQRING SPRLLIK	YASE SIS	RIPSRFSGSGSGTDFTLTINSV ESEDIADYYC	QQSNS WPALT	FGAGTK LEIKR	GGGGSGGGG SGGGGS

	VH						
	FR1	CDR1	FR2	CDR2	FR3	CDR3	FR4
C-7	EVMLVESGPELVKPGASVKISCK KASGYTFS	SYWMN	WMKQRPG KGLEWIG	QIYPGDGET NYNGKFKG	KATLTADKSSSTAYMQLS SSLTSEDSAVYFCAS	FDGYYVDY	WGQGT TLQSS
D-5	QVQLQQSGPELARPWASVKISC CQAFYTFS	RRVHFAIRD DTNYWMQ	WVKQRPGQ QGLEWIG	AIYPGNGDT SYNQKFKG	KALTLTADKSSSTAYMQL LSSLTSEDSAVYFCAR	DPLVY	WGQGT TLTVSS
D-6	QVHVKQSGAELVKPGAAVKVSC CKASGYTFT	SYWMH	WVKQRPGH HGLEWIG	QIYPGDGDT NYNGEFKG	KALTLTVDKSSSTAYMQL LSSLTSEDSAVYFCAS	QSSYVFDY	WGQGT TLTVSS
E-6	EVQLQQSGPELVKPGASVKISC KASGYSFT	DYNMN	WVKQSNGK KSLEWIG	VINPNYGTTS SYNQKFKG	KALTLTVDQSSSTAYMQL LSSLTSEDSAVYYCTR	ENYYGSSY LYYAMDY	WGQGT TVTVSS

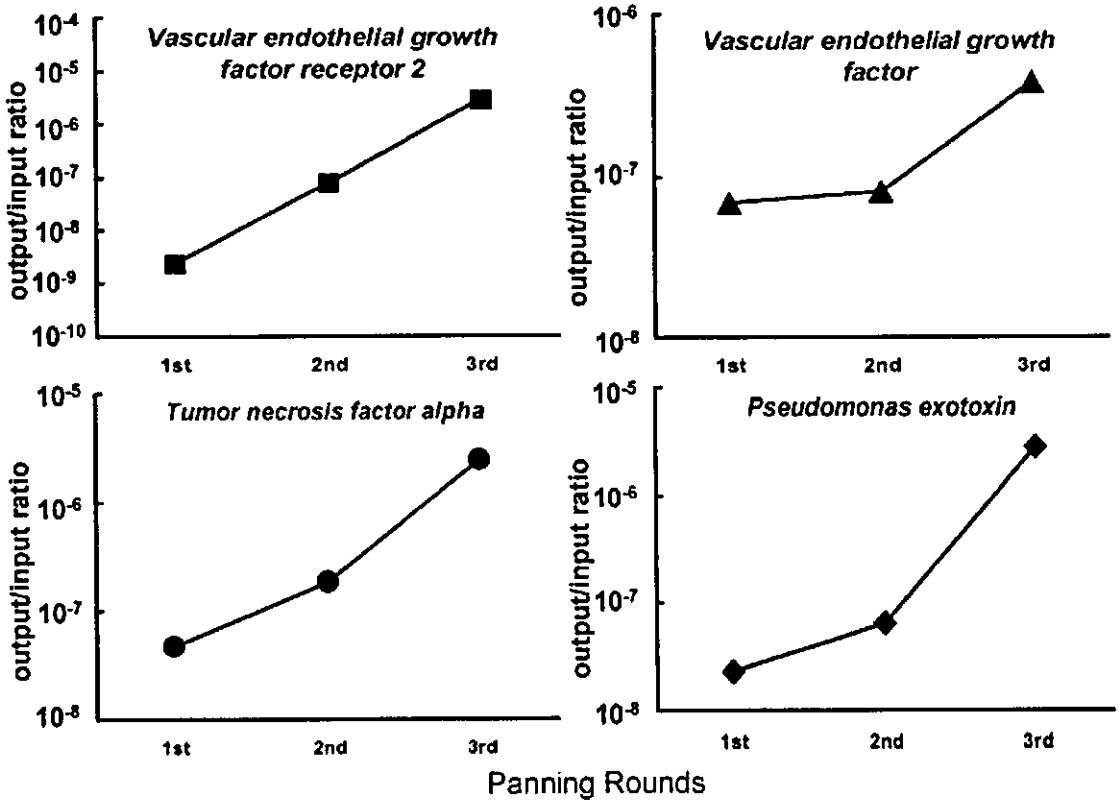

図22 ナイーブ抗体ライブラリを用いた種々抗原に対するscFvの単離

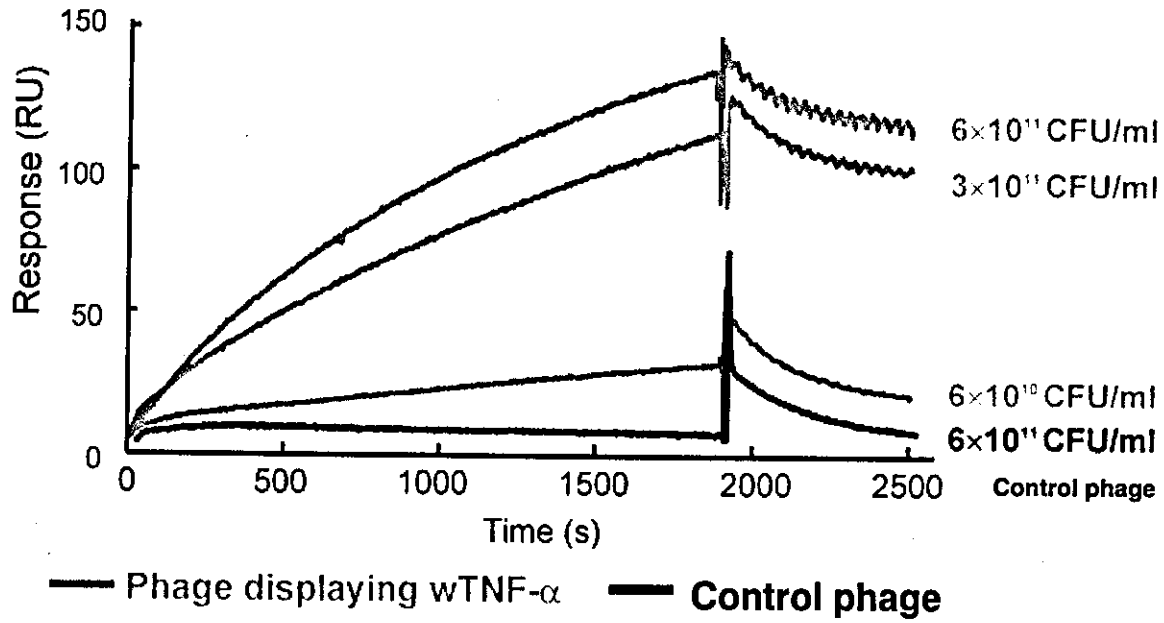

図23 BIAcoreによるパンニングの最適化

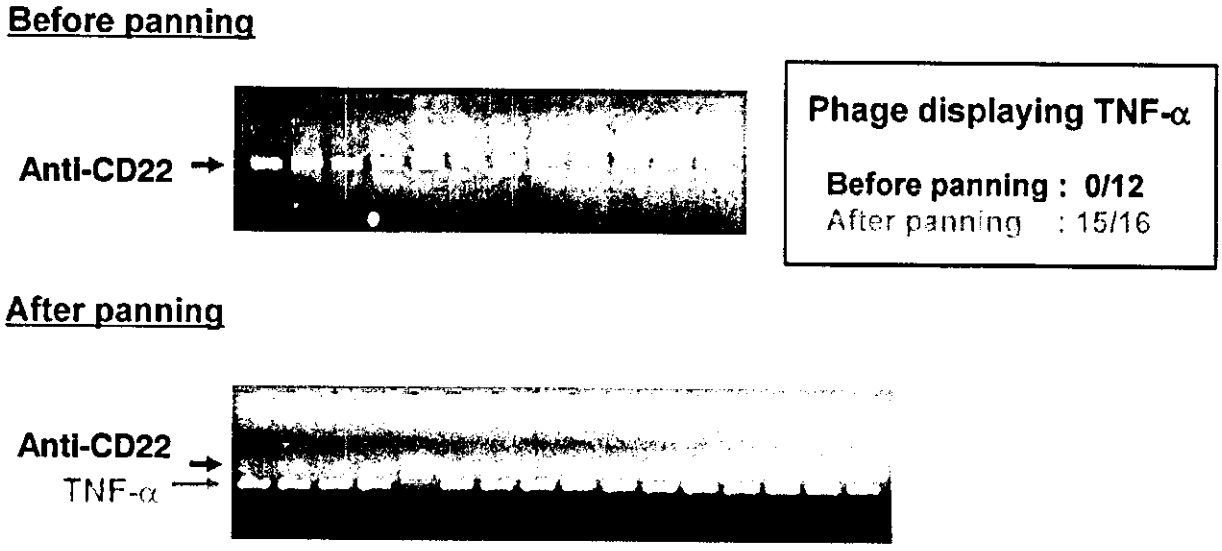

図24 TNFR1に対するパンニングによるwtTNF-α発現ファージの濃縮

表9 wtTNF-αと同等以上の生物活性やレセプター親和性を保持したリジン欠損TNF-α

	Residue positions						
	11	65	90	98	112	128	pI
wTNF-α	Lys	Lys	Lys	Lys	Lys	Lys	7.44
mTNF-α-K90R	Ala	Ser	Arg	Ala	Leu	Thr	4.96
mTNF-α-K90P	Ala	Ser	Pro	Ala	Leu	Thr	4.76

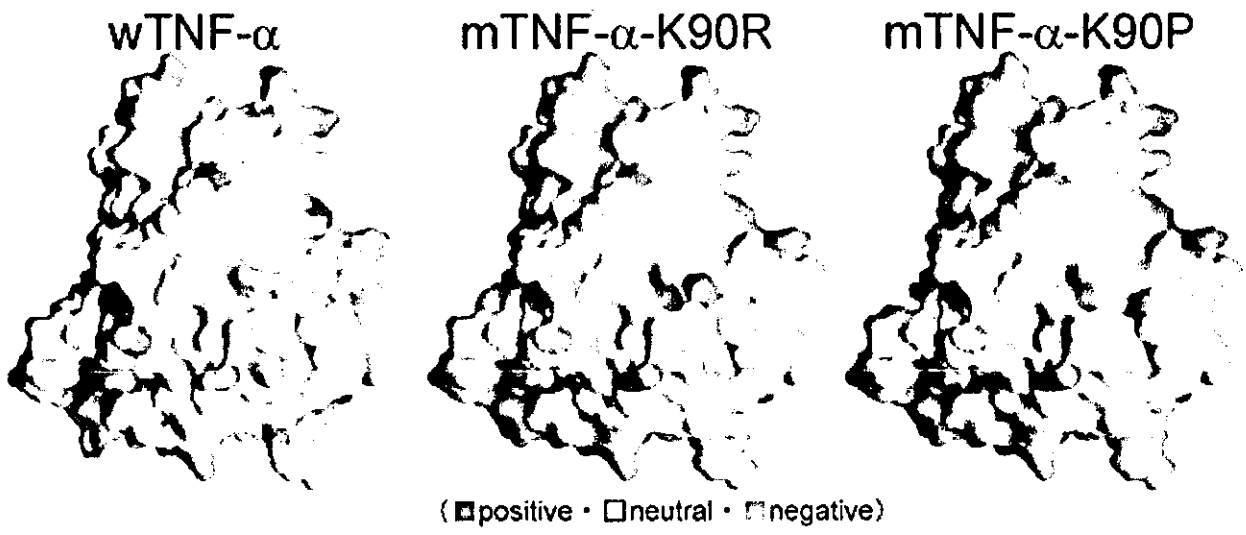

図25 GRASP法によるたんぱく質表面電荷予測

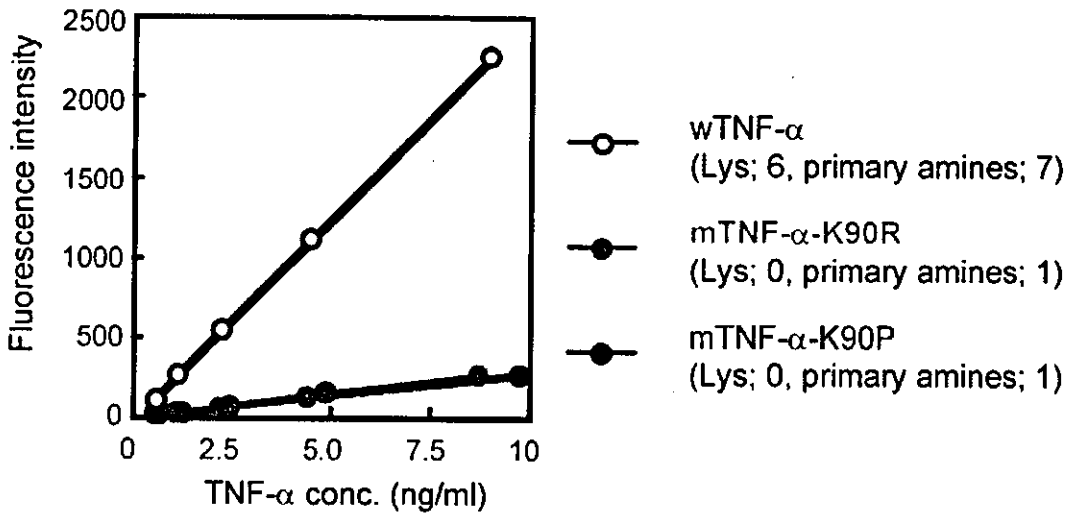

図26 フルオレスカミン法によるTNF-αの1級アミン測定

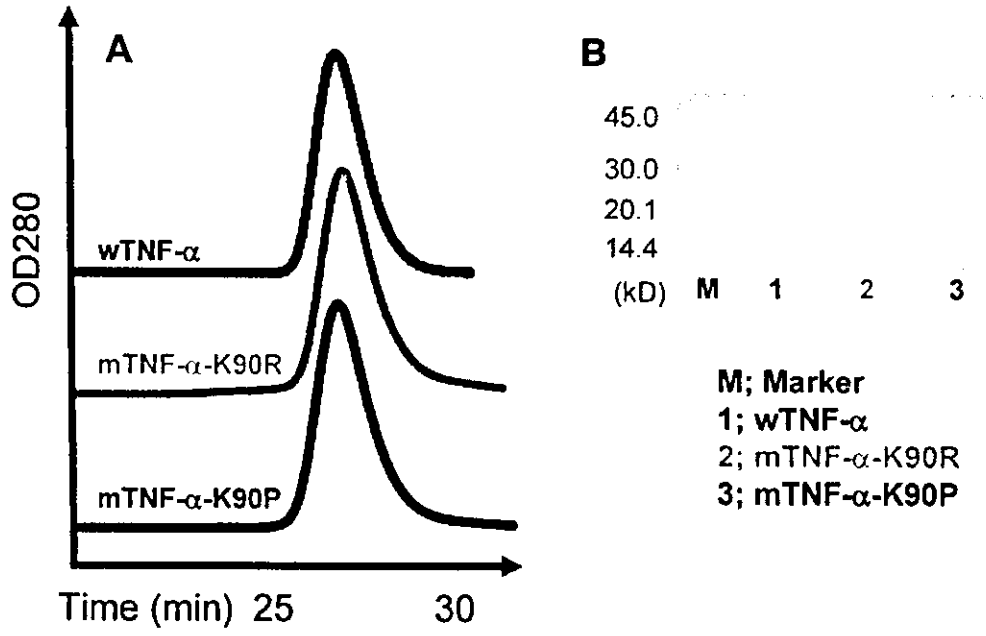

図27 リコンビナント・リジン欠損TNF-αのゲル濾過・SDS-PAGE解析

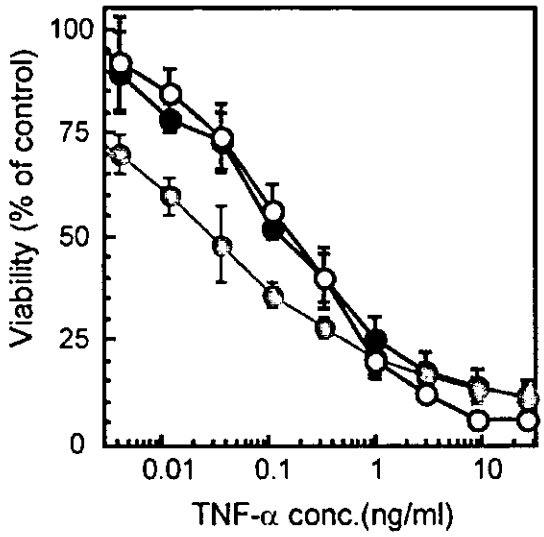

	EC50[1)] (ng/ml)
○ wTNF-α	0.17
◎ mTNF-α-K90R	0.03
● mTNF-α-K90P	0.14

The specific bioactivity of lysine-deficient mTNF-αs was measured by cytotoxic assay using LM cells.
1)The concentration of TNF-α required for 50% inhibition of LM cell viability.

図28A マウスTNFR1を介したリジン欠損TNF-α の生物活性(比活性)

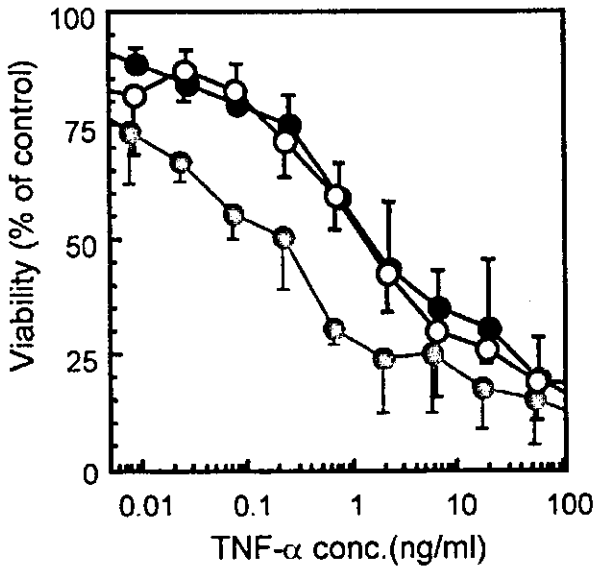

	EC50[1)] (ng/ml)
○ wTNF-α	1.28
◎ mTNF-α-K90R	0.12
● mTNF-α-K90P	1.40

The specific bioactivity of lysine-deficient mTNF-αs was measured by cytotoxic assay using LM cells.
1)The concentration of TNF-α required for 50% inhibition of Hep2 cell viability.

図28B ヒトTNFR1を介したリジン欠損TNF-α の生物活性

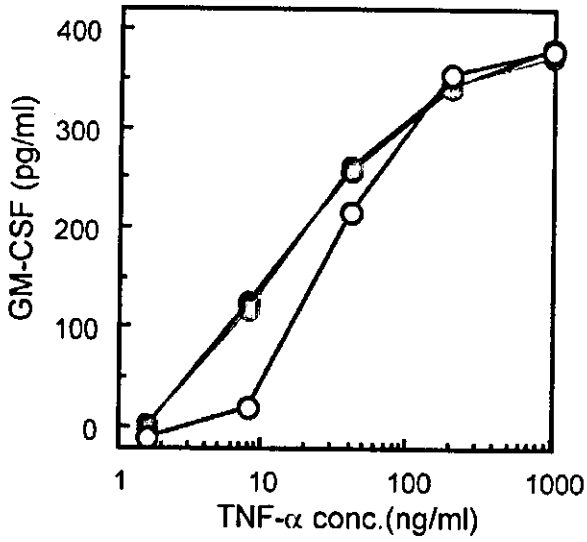

	EC50[1] (ng/ml)
○ wTNF-α	41.5
◐ mTNF-α-K90R	19.9
● mTNF-α-K90P	19.8

1)The values are given as the concentration of TNF-α required to induce secretion of 200pg/ml GM-CSF.

図29 ヒトTNFR2を介したリジン欠損TNF-α の生物活性

表10 リジン欠損TNF-αのヒトTNFR1に対する結合特性(解離定数)

	Ka[1] ($\times10^5 M^{-1}s^{-1}$)	Kd[2] ($\times10^{-4}s^{-1}$)	KD[3] ($\times10^{-10}M$)	Relative[4] (%)
wTNF-α	9.7±0.2	1.94±0.08	1.98±0.04	100
mTNF-α-K90R	11.1±0.1	1.60±0.12	1.44±0.13	138
mTNF-α-K90P	12.0±0.4	1.62±0.22	1.35±0.23	147

1)Association rate constant
2)Dissociation rate constant
3)Equilibrium dissociation constant
4)Relative values for the KD were calculated from the KD(wTNF-α)/KD(lysine-deficient mTNF-α)
Parameters were determined from eqilibrium binding using BIA evaluation 3.0 program

表11 リジン欠損TNF-αのヒトTNFR2に対する結合特性(解離定数)

	Ka[1] ($\times 10^{6} M^{-1}s^{-1}$)	Kd[2] ($\times 10^{-3} s^{-1}$)	KD[3] ($\times 10^{-10} M$)	Relative[4] (%)
wTNF-α	4.09±0.51	1.18±0.24	2.87±0.24	100
mTNF-α-K90R	5.31±0.63	0.99±0.31	1.92±0.80	149
mTNF-α-K90P	5.42±0.85	1.12±0.31	2.16±0.87	133

1)Association rate constant
2)Dissociation rate constant
3)Equilibrium dissociation constant
4)Relative values for the KD were calculated from the KD(wTNF-α)/KD(lysine-deficient mTNF-α)
Parameters were determined from eqilibrium binding using BIA evaluation 3.0 program

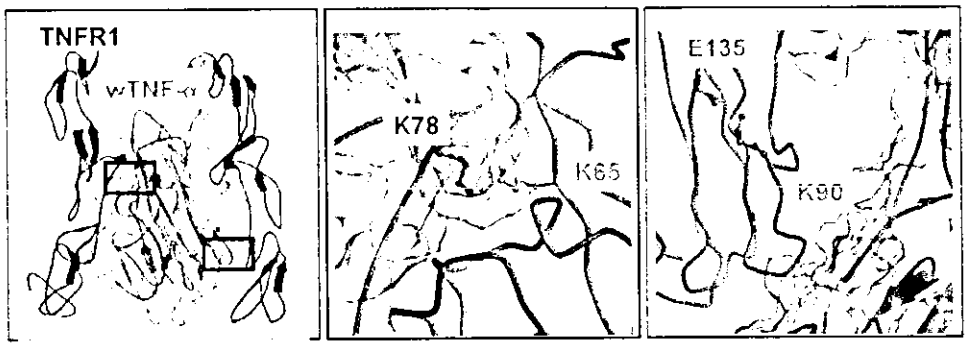

図30 wtTNF-αとヒトTNFR1の結合モデル

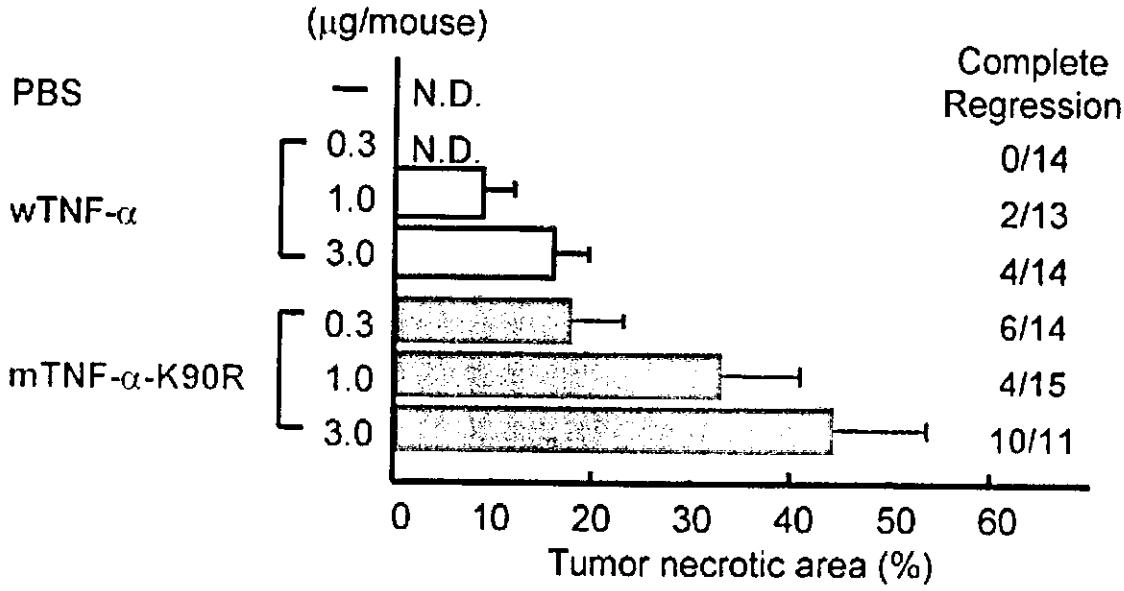

図31 mTNF-α-K90Rの*in vivo*における抗腫瘍効果

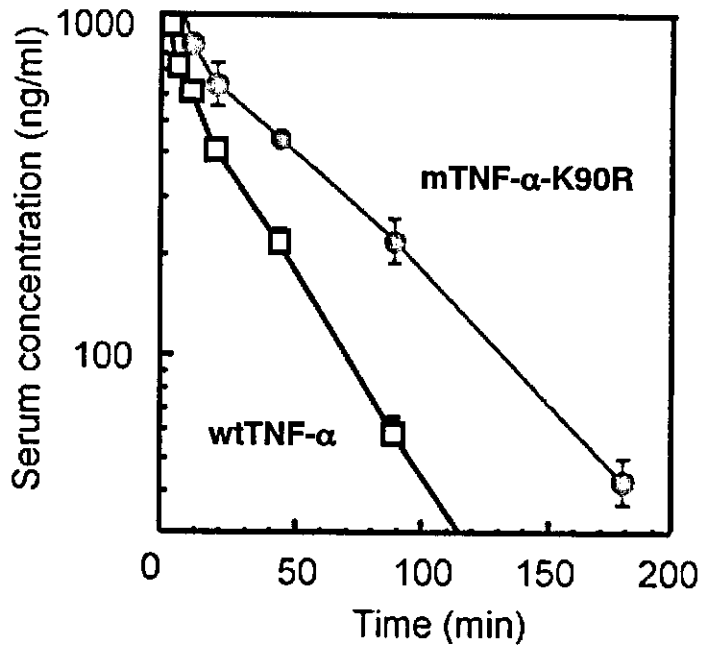

図32 mTNF-α-K90Rの静脈内投与後の血中動態

表12 mTNF-α-K90Rの血中動態パラメーター

	t1/2 (min)	AUC (x10^{3}ng·min/ml)	CLtotal (μl/min)
□ wTNF-α	12 ± 2	28 ± 2	39 ± 4
● mTNF-α-K90R	24 ± 5	62 ± 7	17 ± 2

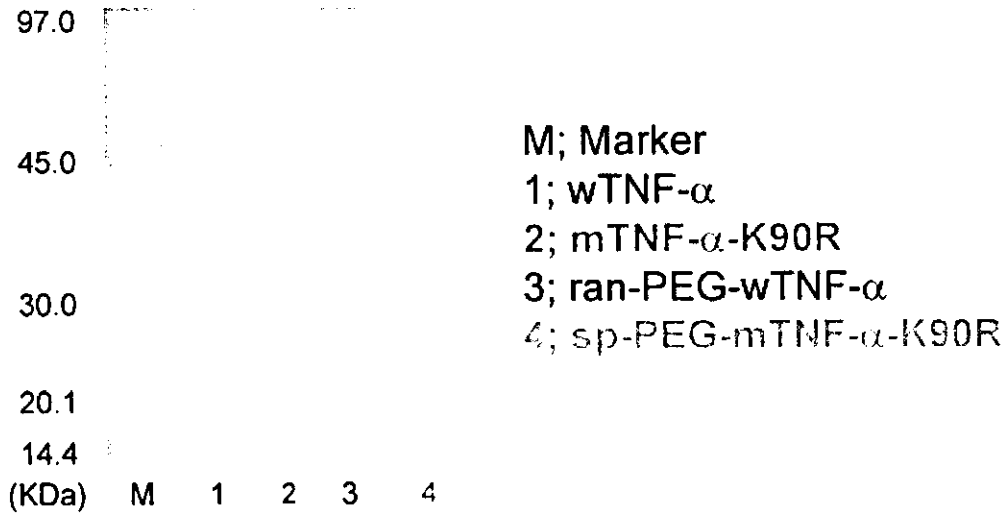

図33 wtTNF-α及びmTNF-α-K90R のPEGylationとこれらのSDS-PAGE解析